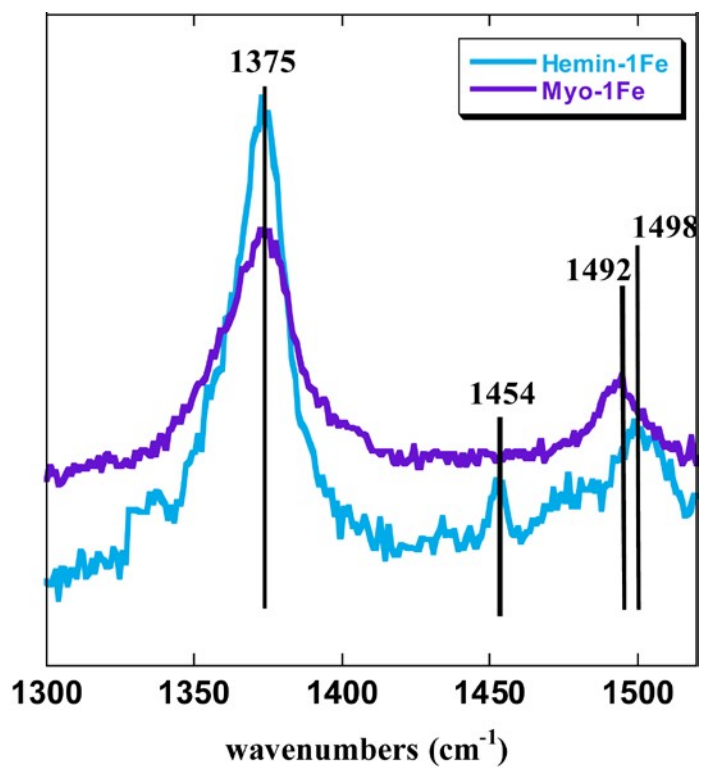


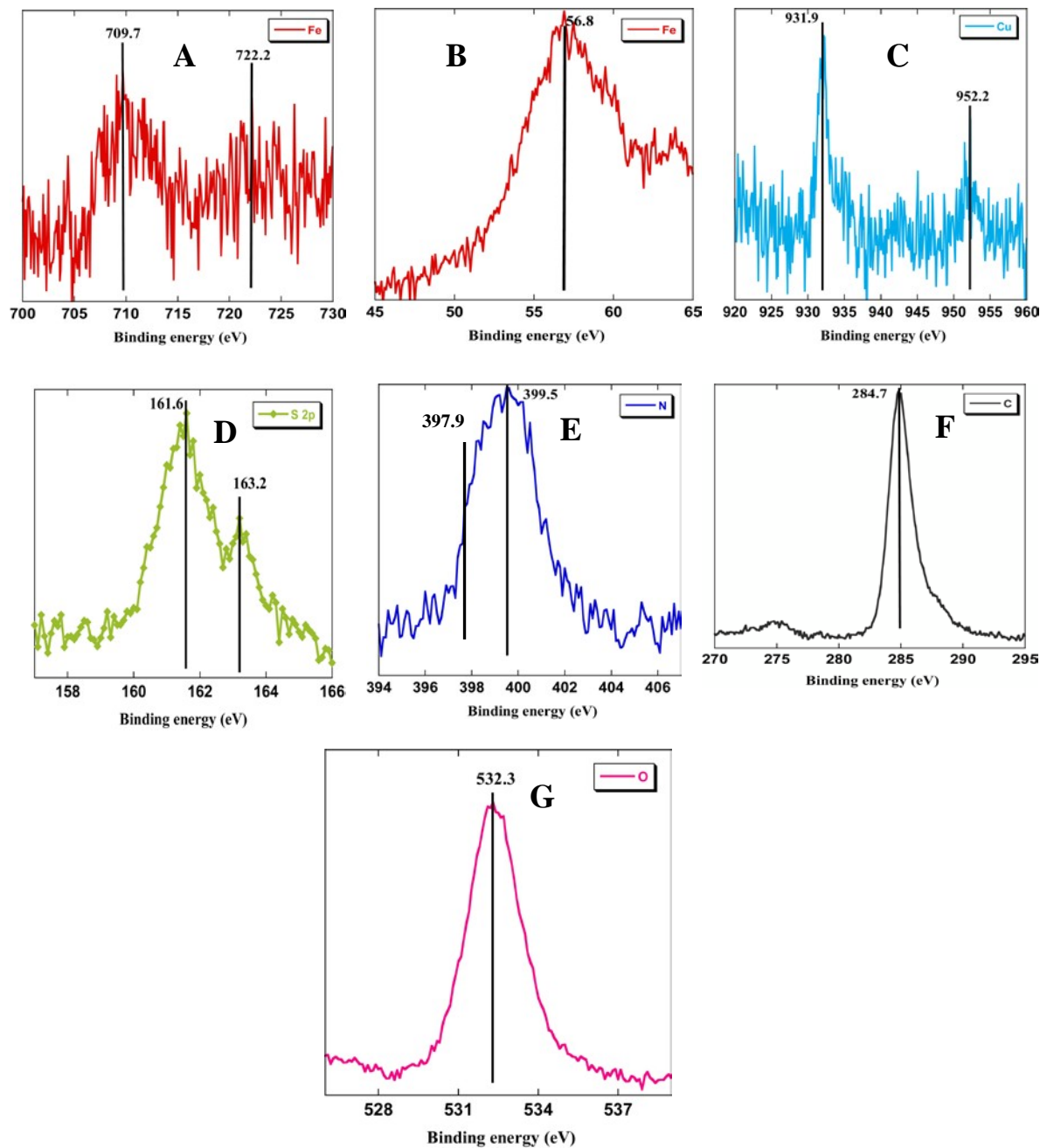
Supplementary Information

SERRS of electrodes bearing Hemin-yne and myoglobin reconstituted with Hemin-yne



Supplementary Figure 1. SERRS spectra of Hemin-yne and myoglobin reconstituted with Hemin-yne in air saturated 100 mM phosphate buffer (pH 7) solution.

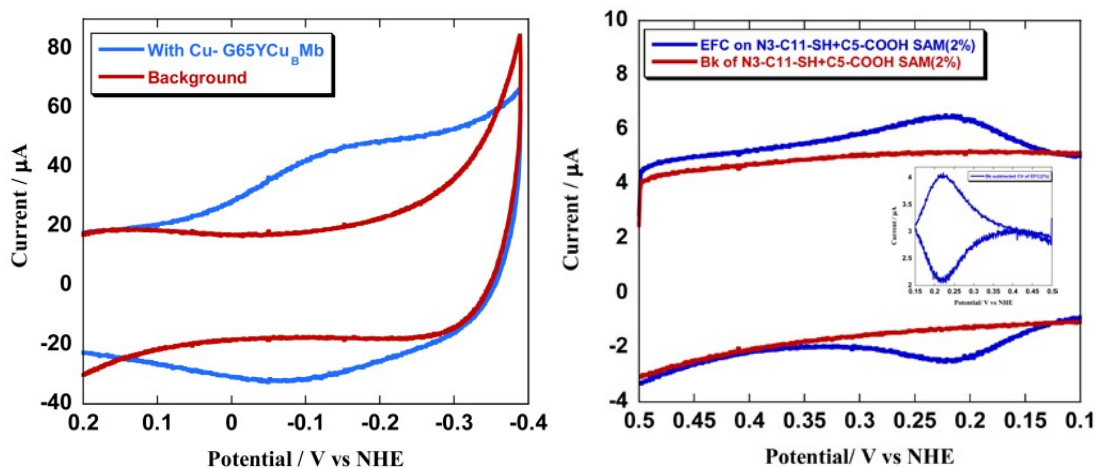
X-ray Photoelectron Spectroscopic data



Supplementary Figure 2. High-resolution XP spectra for G65YCu_BMb (with Cu) mutant immobilized on the SAM covered Au Surface using click reaction. (A) Fe 2p_{3/2}

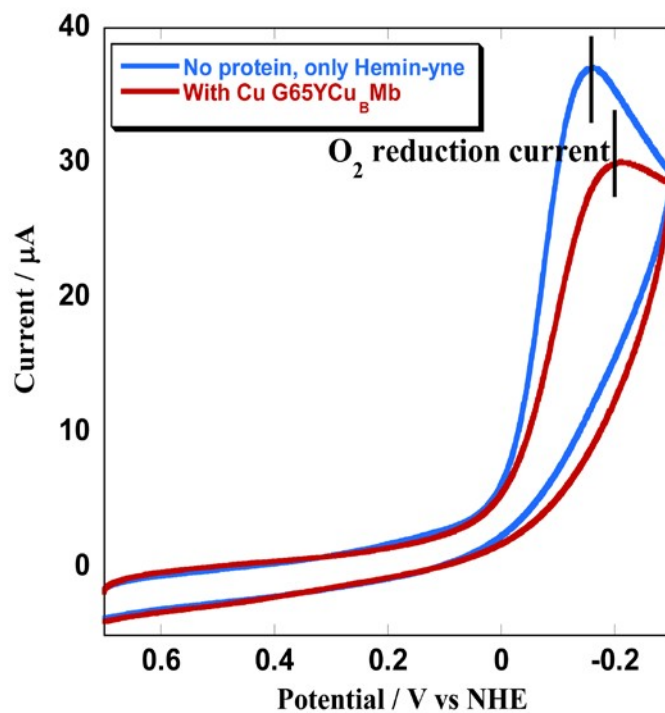
and $2p_{1/2}$ (B) Fe $3p_{3/2}$ (C) Cu $2p_{3/2}$ and $2p_{1/2}$ (D) S $2p_{3/2}$ and $2p_{1/2}$ (E) N $1s_{1/2}$ for triazole linkage (F) C $1s_{1/2}$ (G) O $1s_{1/2}$.

Background subtraction from the CV of the electrode functionalized with G65YCu_BMb protein



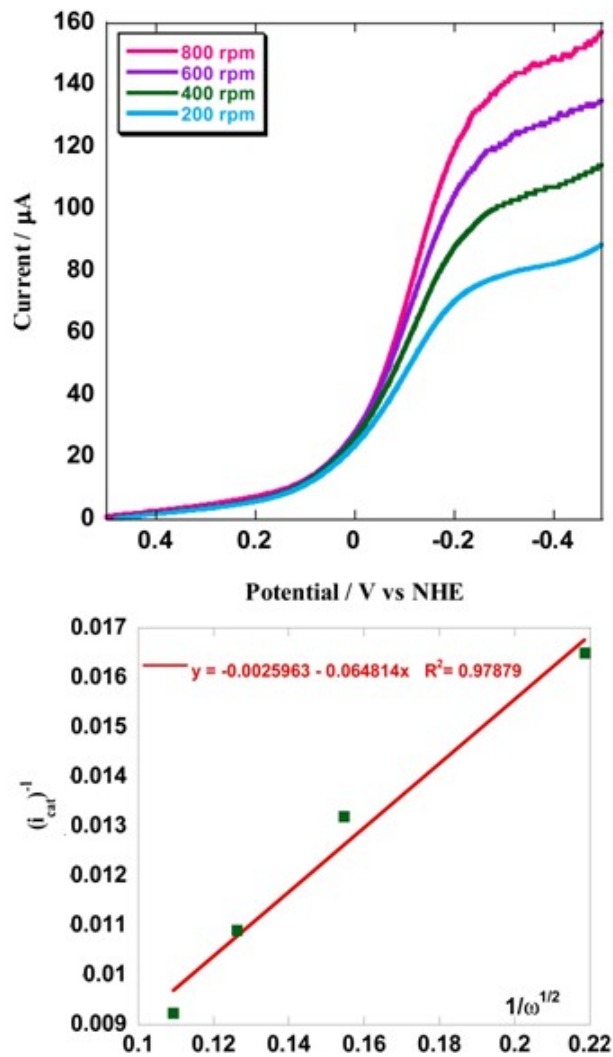
Supplementary Figure 3. (left) Overlay of the CV of the bioelectrode with the background current obtained before protein attachment (right) overlay of the background current with ethynylferrocene attached to the surface having same density of azide instead of the heimin-1Fe.

O₂ Reduction by the Hemin-yne modified surface before and after G65YCu_BMb (with Cu) protein binding



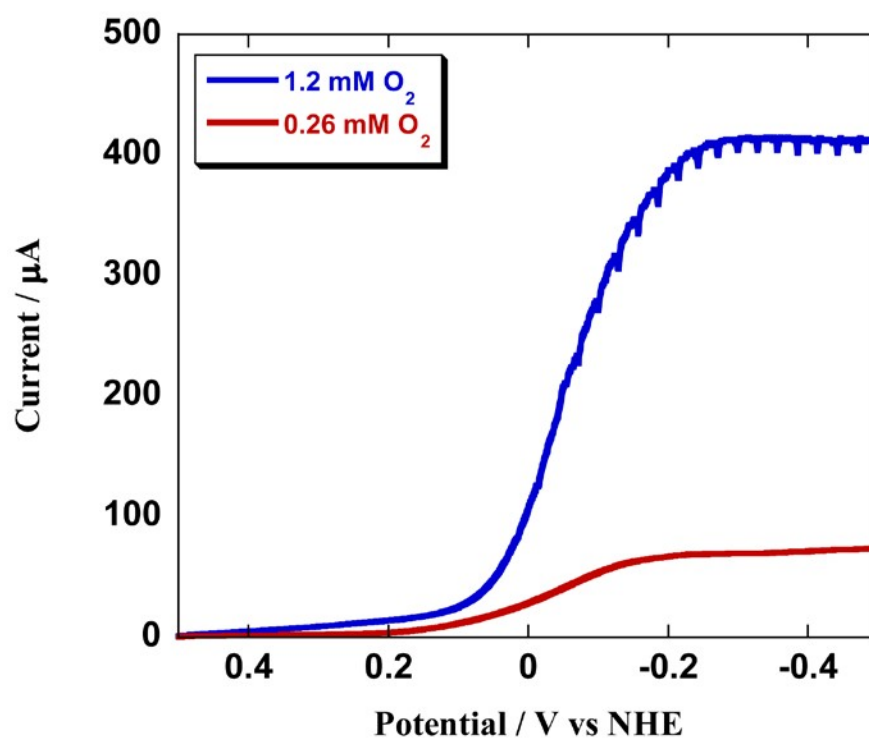
Supplementary Figure 4: Cyclic voltammogram for the O₂ reduction by the Hemin-yne modified surface before (blue) and after G65YCu_BMb (with Cu) protein (red) binding, in 100 mM pH 7 phosphate buffer (air saturated) using Ag/AgCl electrode as reference and Pt as counter electrode.

RDE data



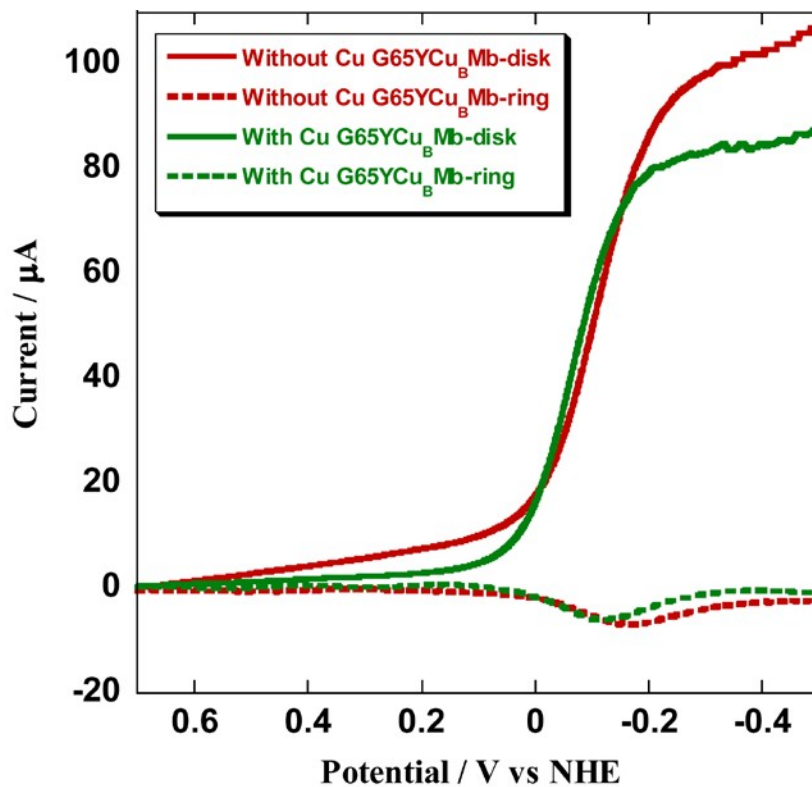
Supplementary Figure 5: Linear sweep voltammogram of G65YCu_BMb (without Cu) modified electrode in air saturated pH7 100 mM phosphate buffer solution at 100 mV/s scan rate and using Ag/AgCl electrode as reference and Pt as counter electrode are plotted at different rotation speed (top). Plot of $(i_{\text{cat}})^{-1}$ at multiple rotation rates with the inverse square root of the angular rotation rate ($\omega^{-1/2}$) is also shown (bottom).

LSV for electrocatalytic ORR at different concentration of O₂



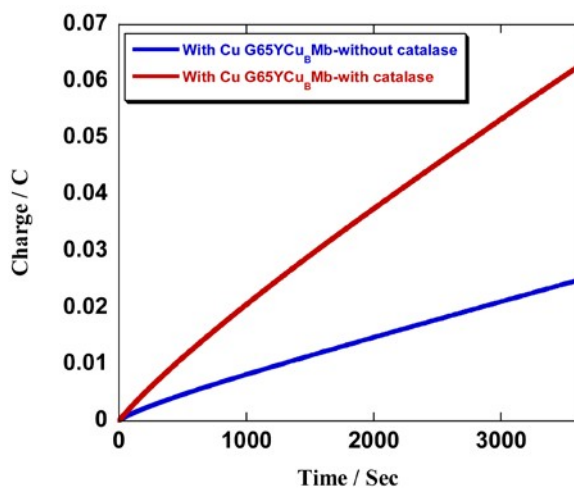
Supplementary Figure 6: LSV for electrocatalytic ORR at different concentration of O₂ at 300 rpm rotation and at 100 mV/s scan rate.

RRDE



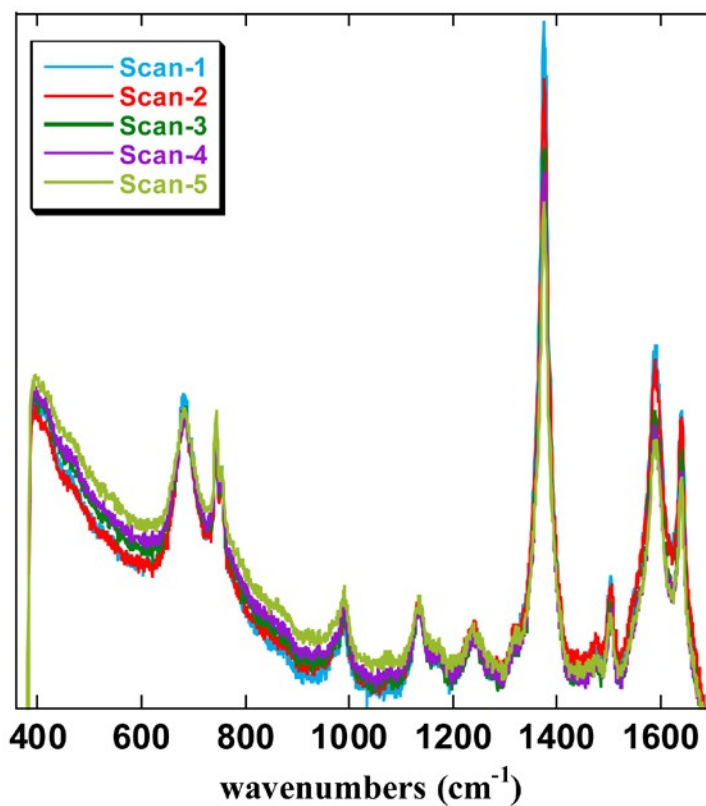
Supplementary Figure 7: Rotating ring disk electrode (RRDE) data of without Cu, G65YCu_BMb (red) and with Cu, G65YCu_BMb (green) at 10 mV/s and at 300 rpm rotation speed in air saturated pH 7 100 mM phosphate buffer using Ag/AgCl electrode as reference and Pt as counter electrode. The Pt current of the data for without Cu, G65YCu_BMb (red) and with Cu, G65YCu_BMb (green) were scaled by a factor of 10 and 15, respectively, for clear presentation.

Degradation of With Cu G65YCu_BMb modified surface on PROS production (both in presence and in absence of catalase)



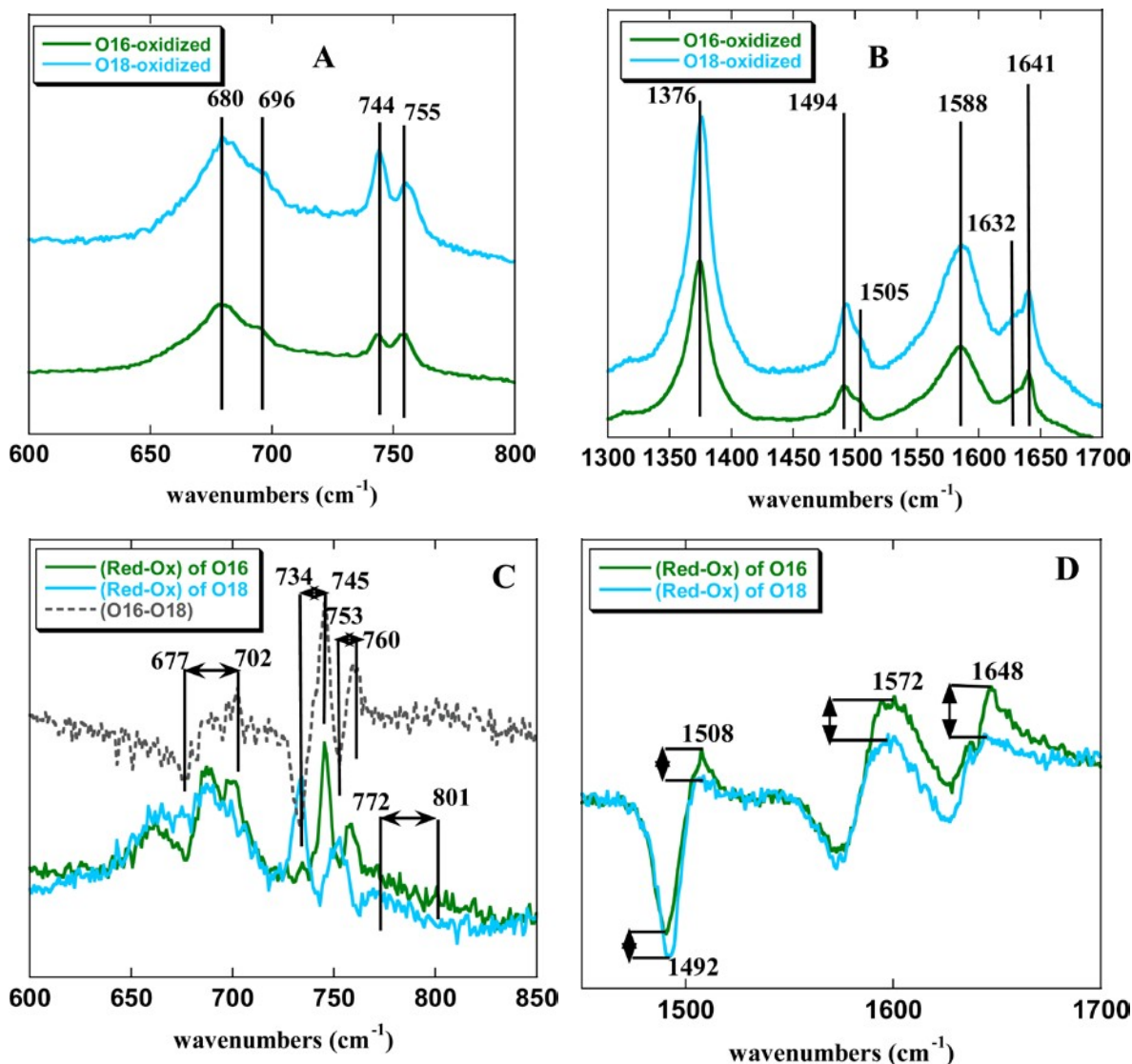
Supplementary Figure 8: Charge vs time plot for the degradation of with Cu G65YCu_BMb modified surface with PROS production (in absence and in presence of 50 μ M catalase in pH 7 phosphate buffer), at 200 rpm rotation and at -0.3 V vs NHE.

Stability of the G65YCu_BMb (with Cu) protein modified surface during electrolysis at -0.4 V vs NHE



Supplementary Figure 9: SERRS-RDE spectra of G65YCu_BMb (with Cu) protein modified surface, collected over 500 seconds during a bulk electrolysis experiment at -0.3 V vs NHE during which the electrode is under continuous rotation (300 rpm). Five scans are performed for 100 seconds each (one LSV is typically 20 seconds), in 100 mM pH 7 phosphate buffer saturated with O¹⁸ isotope, using Ag/AgCl reference electrode and Pt counter electrode.

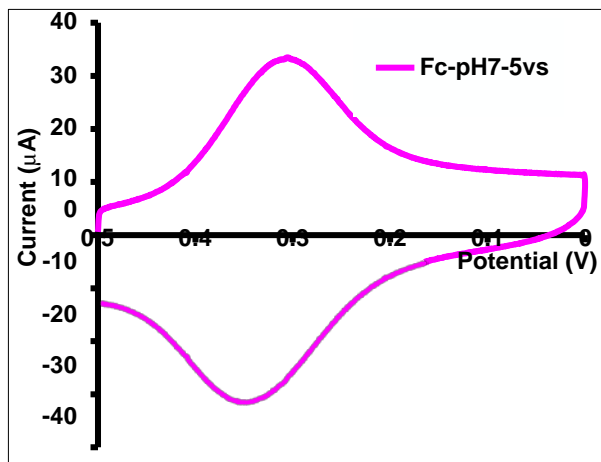
SERRS-RDE data obtained in $^{18}\text{O}_2$ and $^{16}\text{O}_2$ buffer.



Supplementary Figure 10: SERRS-RDE on G65YCu_BMb with Cu, immobilized bioelectrode in the presence of O_2^{16} and O_2^{18} saturated pH 7 phosphate buffer. (A) Oxidized spectra in O_2^{16} and O_2^{18} saturated pH 7 phosphate buffer at low range of wavenumbers (B) Oxidized spectra in O_2^{16} and O_2^{18} saturated pH 7 phosphate buffer at high range of wavenumbers (C) Difference spectra of reduced and oxidized state in O_2^{16} and O_2^{18} saturated pH 7 phosphate buffer at low range of wavenumbers, showing the

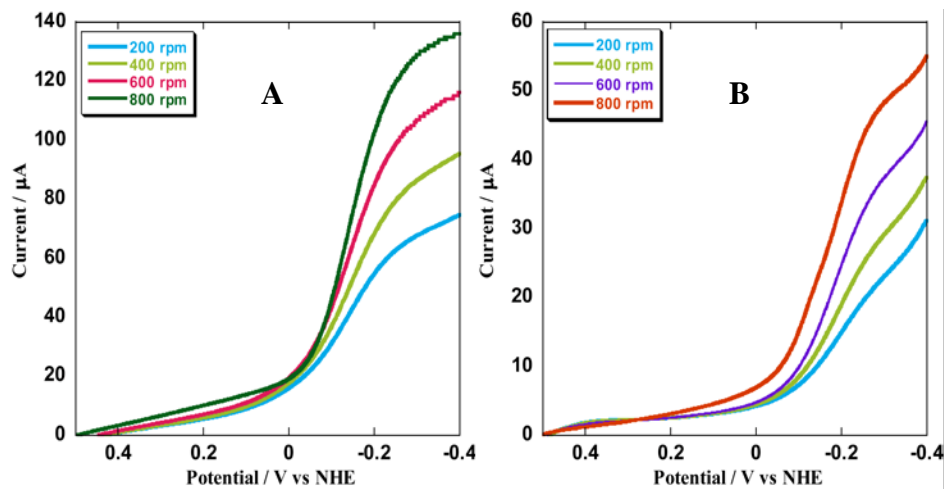
isotopic shift (D) Difference spectra of reduced and oxidized state in O_2^{16} and O_2^{18} saturated pH 7 phosphate buffer at high range of wavenumbers, showing the increase in intensity of the peaks from O_2^{18} to O_2^{16} .

CV of ethynylferrocene attached to the surface modified with the SAM of 1-azidoundecan-11-thiol and 6-mercaptopentanoic acid



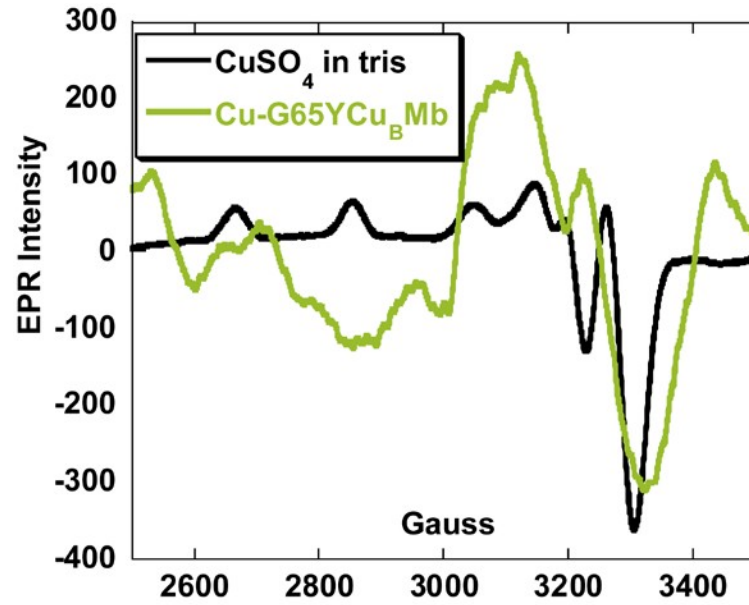
Supplementary Figure 11. CV of ethynylferrocene attached to the surface modified with the SAM of 1-azidoundecan-11-thiol and 6-mercaptopentanoic acid, at 5 V/s scan rate and using Ag/AgCl as the reference electrode and Pt as the counter electrode.

Decay of Hemin-yne, Hemin-yne bound Cu_BMb (no Y65)



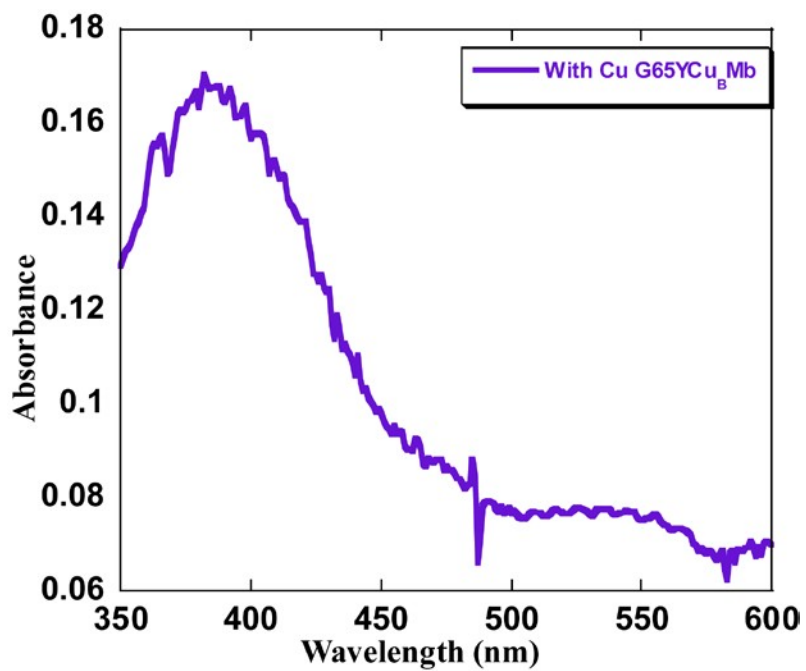
Supplementary Figure 12: Decay of O_2 reduction current at different angular rotation rate for (A) Hemin-yne (B) Hemin-yne bound Mb. Data clearly indicates the rapid decay of these catalysts.

EPR



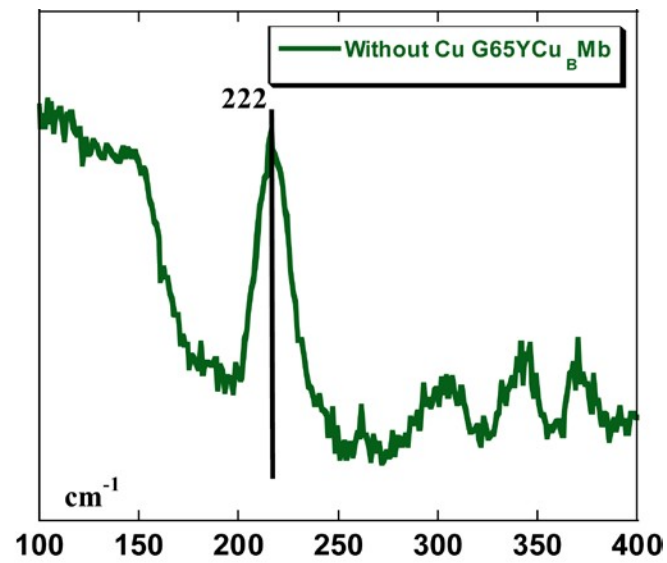
Supplementary Figure 13: EPR spectra of G65YCu_BMb (green) with Cu compared with CuSO₄ (black) in 10 mM pH 7 phosphate buffer.

UV-vis absorption spectra of G65YCu_BMb with Cu on the Au surface



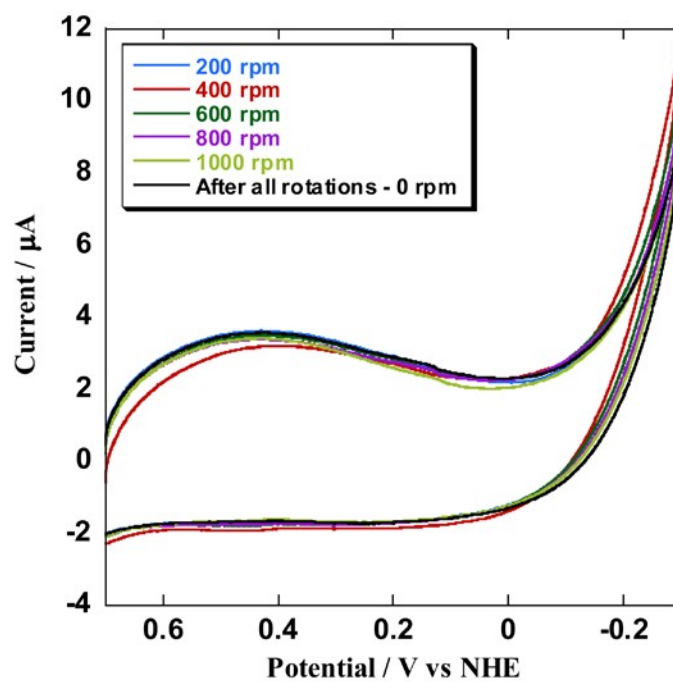
Supplementary Figure 14: Uv-vis absorption spectra of G65YCu_BMb with Cu in 10mM pH 7 phosphate buffer.

Fe-His stretch



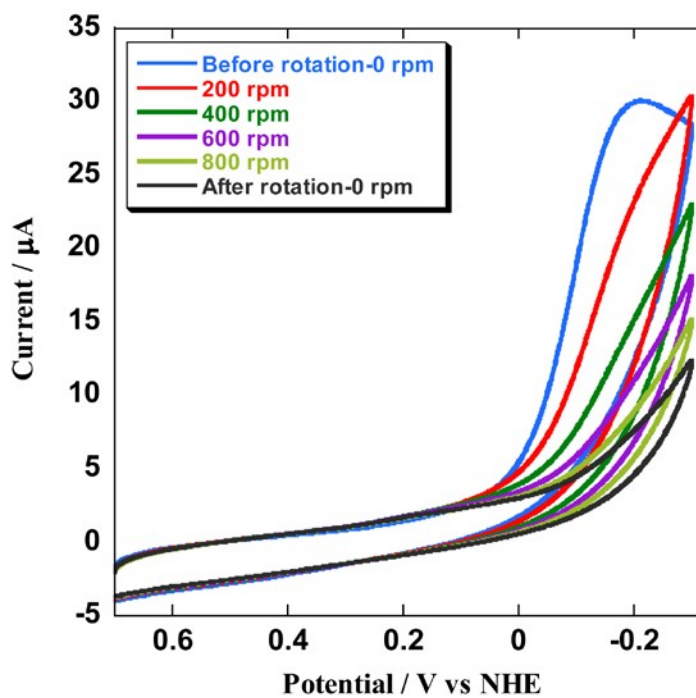
Supplementary Figure 15: Resonance Raman spectra of the homogenous solution of G65YCu_BMb (green) with Cu indicating the Fe-His stretching frequency at 220 cm⁻¹.

Stability of the mixed SAM of 1-azidoundecan-11-thiol and 6-mercaptohexanoic acid after rotations



Supplementary Figure 16: Cyclic voltammogram of the background current of mixed SAM of 1-azidoundecan-11-thiol and 6-mercaptohexanoic acid, in 100 mM pH 7 phosphate buffer at after rotating the electrode at different rotation rates. (Ag/AgCl reference and Pt counter electrode)

Stability of the G65YCu_BMb (with Cu) protein modified surface after rotations



Supplementary Figure 17: Cyclic voltammogram of the G65YCu_BMb (with Cu) protein modified surface, in 100 mM pH 7 phosphate buffer at different rotation rate using Ag/AgCl electrode as reference and Pt as counter electrode.

Supplementary Table 1. XPS data of G65YCu_BMb (with Cu) modified Au electrode

| Binding Energies (eV) | | |
|------------------------------|-------------------|--------------|
| Fe | 2p _{3/2} | 709.7 |
| | 2p _{1/2} | 722.2 |
| | 3p _{3/2} | 56.8 |
| Cu | 2p _{3/2} | 931.1 |
| | 2p _{1/2} | 952.2 |
| S^I | 2p _{3/2} | 161.6 |
| | 2p _{1/2} | 163.7 |
| N | 1s _{1/2} | 397.9, 399.5 |
| C | 1s _{1/2} | 284.7, 287.8 |
| O^I | 1s _{1/2} | 532.3 |

Supplementary Reference

1. Yuan, S. J.; Pehkonen, S. O., Surface characterization and corrosion behavior of 70/30 Cu-Ni alloy in pristine and sulfide-containing simulated seawater. *Corros. Sci.* **49**, (3), 1276-1304, (2007).